

Studying Ionic Motion in Tetrahydroxoborate Sodalite by Second Moment Analysis Using $^{23}\text{Na}\{^{11}\text{B}\}$ Rotational Echo Double Resonance Data

Hubert Koller* and Martin Kalwei

*Institut für Physikalische Chemie, Westfälische Wilhelms-Universität, Schlossplatz 4/7,
48149 Münster, Germany*

Received: April 29, 2003; In Final Form: October 8, 2003

Rotational echo double resonance (REDOR) is used to analyze ionic motion in tetrahydroxoborate sodalite, which can be regarded as a model system for rotor phases. The motional averaging of $^{11}\text{B}-^1\text{H}$ and $^{23}\text{Na}-^{11}\text{B}$ dipole interactions probes both the reorientation of the tetrahydroxoborate anions and the sodium motion, respectively. To this end, REDOR data from multiple-spin systems with quadrupolar nuclei have to be analyzed quantitatively, and the underlying theoretical model is presented. The results show that simple ^{23}Na NMR line narrowing analysis can lead to misleading conclusions, and the REDOR method is a valuable tool to investigate local motion in ionic systems.

Introduction

The mechanism of local ionic motion is of fundamental interest for a better understanding of ion conductivities and other materials properties. Solid state nuclear magnetic resonance techniques have been frequently used to study the motional characteristics of the involved species in all kinds of materials.^{1,2} The sensitivity of these methods on motion rely on anisotropic nuclear spin interactions, which become dynamically affected if there is motion in the system. Anisotropic nuclear spin interactions, such as the chemical shift anisotropy, the nuclear quadrupole interaction, and the nuclear dipole–dipole interaction are very useful sources of structural and dynamical information. Detailed mechanistic dynamic information is usually accessible, when the tensors of these anisotropic interactions are partially averaged out by a restricted motional process. However, the anisotropic spin interactions give not always a clear indication about which part of the structure is moving. An important example is the electric quadrupole interaction, which is an interaction between the nuclear electric quadrupole moment of a nuclear spin and a local electric field gradient. If this interaction is averaged out by motional processes, then it is not clear whether the nuclear spin, which is under observation, is moving itself or whether the surrounding neighbors are mobile and thus modify the electric field gradient to a reduced value. In addition, a decreased quadrupole interaction could also be caused by an increased site symmetry, because the mobile environment allows for small dislocations of the quadrupolar spin with a lower field gradient. Therefore, it is desirable to have alternatives at hand that prove or disprove a motional model based on another anisotropic spin interaction, such as the magnetic dipole interaction. The basic idea of this work is that information on the spatial orientation of ions and their dynamical reorientation can be obtained by the heteronuclear dipole interaction. The advantage of this interaction is that it can be measured selectively for a chosen spin system, which reduces the number of unknown variables.

This work shows how the dipolar interaction can be exploited for dynamic analysis in multiple-spin systems when quadrupolar

nuclei are involved. To this end, we have chosen the tetrahydroxoborate sodalite (from here on labeled “BOSO”) with a unit cell composition of $[\text{Na}_4\text{B}(\text{OH})_4]_2[\text{Si}_6\text{Al}_6\text{O}_{24}]$. The structure contains $\text{Na}_4[\text{B}(\text{OH})_4]^{3+}$ clusters, which are isolated in an aluminosilicate zeolite matrix, and thus represents a model system of the so-called rotor phases.

The sodalite framework is composed of a space-filling packing of 4^66^8 (sodalite) cages with alternating $\text{AlO}_{4/2}^-$ and $\text{SiO}_{4/2}$ tetrahedra. Figure 1 illustrates a sodalite cage by a wire model where only the corners between the Si and Al centers are shown and framework oxygen atoms of the cage are neglected. All of the cages of this sodalite are filled with four sodium cations in a tetrahedral arrangement at positions near six-rings of the sodalite cage and one orientationally disordered $\text{B}(\text{OH})_4^-$ anion (Figure 1).³ Three of the sodium ions balance the charge of the aluminosilicate framework. Also shown in Figure 1 are the positions of the sodium cations in adjacent cages, which are at the alternate six-rings. BOSO shows a phase transition near room temperature. Motional processes are presumed to be thermally activated in the high-temperature phase, but to date, this motion has not been further characterized. The position of the boron atom has been refined slightly off-center, which leads to 24 possible symmetry-equivalent sites in space group $P43n$.³

In the present study, the motion of $\text{B}(\text{OH})_4^-$ anions and the surrounding sodium cations in the sodalite cages have been investigated by solid-state NMR techniques. The $^{11}\text{B}-^1\text{H}$ and $^{23}\text{Na}-^{11}\text{B}$ dipolar interactions are used as probes for the motion of the $\text{B}(\text{OH})_4^-$ anions and the Na^+ cations, respectively. This approach is feasible, because the boron atoms are trapped at or close to the center of the sodalite cage, and cannot undergo any appreciable movements (local “vibrations” can be well neglected for the further analysis).

In 1989, rotational echo double resonance (REDOR) was introduced by Gullion and Schaefer,⁴ and it became a prominent tool to investigate heteronuclear dipole interactions in solids from which model-free and quantitative distance information is available under high-resolution conditions. The most challenging limitation of the REDOR method is that it can only be analytically analyzed when small spin systems, ideally isolated

* Corresponding author. Phone: +49 251 8323448. Fax: +49 251 8329159. E-mail: hkoller@uni-muenster.de.

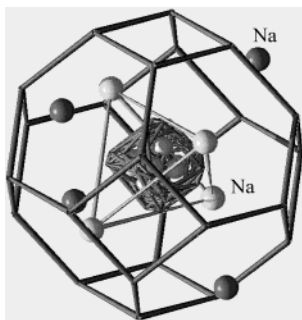


Figure 1. Sketch of the sodalite cage structure with four tetrahedrally arranged sodium cations within and outside of the cage of tetrahydroxoborate sodalite (BOSO). The tetrahydroxoborate anion is located close to the center of the cage, and it is illustrated as a cartoon that emphasizes the orientational disorder.

two-spin- $1/2$ pairs, are involved. Additional problems are encountered when quadrupolar nuclei and motional processes have to be dealt with. These are serious limitations for the application of REDOR to inorganic solids, since isolated two-spin pairs are extremely rare and quadrupolar nuclei are abundant in many systems. Bertmer and Eckert⁵ have proposed that the limitation to small nuclear spin systems can be overcome by analyzing REDOR data in terms of second moment information (for details see below). The purpose of this work is to demonstrate the usefulness of REDOR when large spin systems of quadrupolar nuclei and even motional processes are present. It will be shown that this approach is in fact successful and some details of the motion of the ions in the sodalite structure can be obtained. To this end, a combination of several solid-state NMR methods has been applied, including REDOR analysis of the dipolar interactions involving all of the constituent ^1H , ^{11}B , ^{23}Na , and ^{27}Al nuclei. It will be clearly shown that ^{23}Na solid-state NMR line narrowing alone does not provide a conclusive proof for high mobility of the cations.

Theoretical Section

The REDOR experiment is carried out in two steps. Here, we used the classical version that was originally introduced by Gullion et al.,⁴ where the intensities of the observed spins, S_0 , are measured with rotor-synchronized spin-echo sequences. In the second step, the same spin-echo experiment is repeated, but now π pulses for the coupling nuclei are transmitted at every half rotor period. Each of these pulses leads to an inversion of the sign of the heteronuclear dipolar coupling constant if the $m = |1/2\rangle \leftrightarrow m = |-1/2\rangle$ transition is excited selectively. As a consequence, a dephasing, Φ , occurs due to the reintroduced heteronuclear dipolar interaction, and this effect leads to an attenuated echo intensity, S . The normalized intensity difference is measured as a function of spin-echo evolution time (number of rotor cycles, N_c). For a two-spin system, one obtains⁴

$$\frac{S_0 - S}{S_0} = \frac{\Delta S}{S_0} = 1 - \cos \Phi \quad (1')$$

or for a powder average,

$$\frac{S_0 - S}{S_0} = \frac{\Delta S}{S_0} = 1 - \frac{1}{4\pi} \int_0^{2\pi} \int_0^\pi \sin \beta \cos[\Phi(D, N_c, T_r)] d\beta d\alpha \quad (1)$$

$$\Phi(D, N_c, T_r) = \pm 4\sqrt{2} N_c D T_r \sin \beta \cos \beta \sin \alpha \quad (2)$$

The shape of this “REDOR curve” is a measure for the

heteronuclear dipole interaction between the two nuclei. α and β are the polar angles of the dipolar axis with respect to the rotor frame, D is the dipolar coupling constant, and T_r is the rotor period.

To date, an analytical solution of the integral does not exist, and the solution is usually found by an analytical approximation⁶ using Bessel functions, $J_k(x)$:

$$\frac{\Delta S}{S_0} = 1 - [J_0(\sqrt{2}\lambda)]^2 + 2 \sum_{k=1}^{\infty} \frac{1}{16k^2 - 1} [J_k(\sqrt{2}\lambda)]^2 \quad (3)$$

with

$$J_k(x) = x^k \sum_{m=0}^{\infty} \frac{(-1)^m x^{2m}}{2^{2m+k} m! (k+m)!} \quad (4)$$

and $\lambda = N_c T_r D$.

The sum in eq 4 converges usually after very few terms. If the dephasing π pulses are transmitted on a noninteger quadrupole nucleus, then other spin states, for example, $m = |\pm 3/2\rangle$, $|\pm 5/2\rangle$, $|\pm 7/2\rangle$, ..., can contribute to the dephasing. The change of the spin state by a single-quantum transition then changes the dipole coupling constant and thus the dephasing effect by an additional factor $2|m|$.^{7,8} This means for ^1H – ^{11}B , or ^{23}Na – ^{11}B REDOR ($I(^{11}\text{B}) = 3/2$) that the REDOR curve of an isolated two-spin system is composed of two contributions

$$\frac{\Delta S}{S_0} = 1/2 (2 - \cos \Phi_D - \cos \Phi_{D'=3D}) \quad (5)$$

A further simplification⁵ of eq 1 is achieved if the cosine term is replaced by a power series, which, with truncation after the second term, leads to

$$\frac{\Delta S}{S_0} = 1 - \frac{1}{4\pi} \int_0^{2\pi} \int_0^\pi \sin \beta \left(1 - \frac{\Phi^2}{2}\right) d\beta d\alpha \quad (6)$$

This integral can now be solved, and the extension to n nuclear pairs yields

$$\frac{\Delta S}{S_0} = \frac{16}{15} (N_c T_r)^2 [D_1^2 + D_2^2 + \dots + D_n^2] \quad (7)$$

The summation of squared dipole coupling constants can be replaced by the second moment of the heteronuclear dipole interaction, M_2

$$M_2 = \frac{4}{15} \left(\frac{\mu_0}{4\pi}\right)^2 \gamma_I^2 \gamma_S^2 \hbar^2 S(S+1) \sum_{i>j} r_{ij}^{-6} = \frac{16\pi^2}{15} S(S+1) \sum_{i>j} D_{ij}^2 \quad (8)$$

to result in⁵

$$\frac{\Delta S}{S_0} = \frac{1}{\pi^2 S(S+1)} (N_c T_r)^2 M_2 \quad (9)$$

This equation is an approximation of eq 1 because of the truncation of the power series in eq 6. Bertmer and Eckert have shown⁵ that the consideration of higher terms is not recommended because the relative orientations of multiple spin pairs, which are inaccessible for unknown structures, need then to be included. However, for small evolution times (or for $\Delta S/S_0 <$

0.2), eq 9 is a very useful approximation to analyze REDOR data of multiple spin systems. For quadrupole nuclei, this model has also to be modified, as already shown in eq 5 for spin- $1/2$ systems. Since $M_2 \sim D^2$, it follows for $I = 3/2$ nuclei that

$$\frac{\Delta S}{S_0} = \frac{1}{2} \left(\frac{1}{\pi^2 S(S+1)} (N_c T_r)^2 M_2 + \frac{3^2}{\pi^2 S(S+1)} (N_c T_r)^2 M_2 \right) = \frac{5}{\pi^2 S(S+1)} (N_c T_r)^2 M_2 \quad (10)$$

The first summation term is for spin state $m = |1/2\rangle$, and the second term is for $m = |3/2\rangle$. The experimental dipolar second moments extracted in this way serve as useful parameters, which can then be further analyzed in terms of motion. The dynamic averaging of the heteronuclear dipole interaction, and thus the second moment averaging, is taken into account by standard procedures.⁹

Experimental Section

Materials. The tetrahydroxoborate sodalite was made according to the following procedure:¹⁰ 1.92 g of quartz (Fluka), 1.63 g of aluminum oxide (Merck), 11.82 g of sodium hydroxide (Aldrich), and 2.80 g of ^{11}B -boron oxide (99% enriched, Aldrich) were mixed in 34 mL of water. ^{11}B -enriched boron oxide was used, because the same sample was also investigated by quasielastic neutron scattering experiments, which will be reported elsewhere. All oxides were finely ground before use. The suspension was placed in a stainless steel autoclave with a 50 mL Teflon insert and was heated for 6 days at 180 °C while the container was rotated by ~ 30 rpm. The material was collected by filtration, washed with water, and dried at 60 °C. D_2O was used instead of H_2O for the synthesis of the deuterated tetrahydroxoborate sodalite. The sodalite material was characterized by X-ray powder diffraction, and it was confirmed to be pure.

NMR. All ^1H , ^{27}Al , ^{23}Na , and ^{11}B MAS, ^{23}Na MQMAS, and all double resonance NMR experiments were performed on a Bruker DSX-500 NMR spectrometer operating at a magnetic field of $B_0 = 11.7$ T using a 4 mm triple resonance MAS probehead from Bruker. Spinning speeds between 5 and 12 kHz were applied. The radio frequency (rf) fields for all experiments were between 50 and 62.5 kHz, except for the ^{23}Na MQMAS experiment, where we used a rf field of 125 kHz for the hard pulses and 20 kHz for the soft pulses. The rf pulses in the REDOR experiments were carefully calibrated by an oscilloscope to ensure that ^{11}B pulse conditions in ^{23}Na – ^{11}B and ^{27}Al – ^{11}B double resonance experiments were the same. The ^{23}Na MAS NMR spectrum was simulated using the WINFIT software from Bruker. The reference samples for chemical shift calibration were TMS for ^1H NMR measurements, $\text{BF}_3 \cdot \text{O}(\text{C}_2\text{H}_5)_2$ for ^{11}B NMR measurements and 1 M aqueous solutions of NaCl and AlCl_3 for ^{23}Na NMR and ^{27}Al NMR measurements. The static ^2H NMR spectra were recorded on an Bruker CXP300 operating at 7.1 T. For the acquisition, we used the $90^\circ_x - \tau - 90^\circ_y - \tau - \text{solid} - \text{echo}$ experiment with $\tau = 20$ μs and a 90° pulse length of 8 μs . ^{23}Na MQMAS NMR experiments were carried out with a three-pulse sequence¹¹ using an rf field of 125 kHz for the hard and 20 kHz for the soft pulses.

Results and Discussion

Figure 2 shows ^{23}Na MAS NMR spectra of BOSO at various temperatures around the phase transition at 303 K. The low-

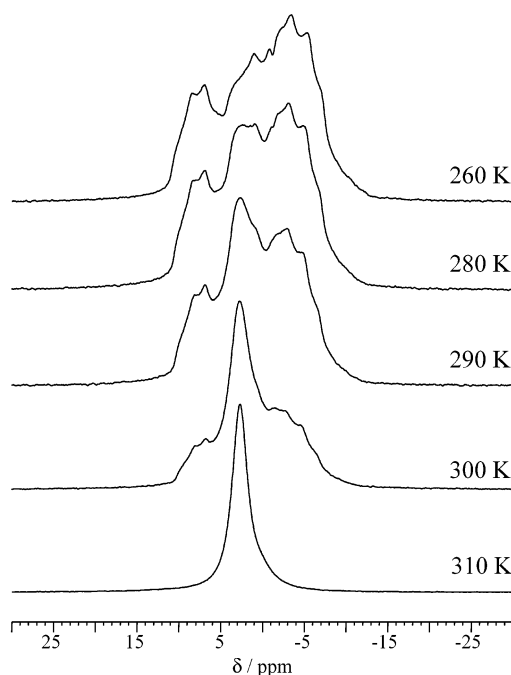


Figure 2. ^{23}Na MAS NMR spectra of BOSO at various temperatures.

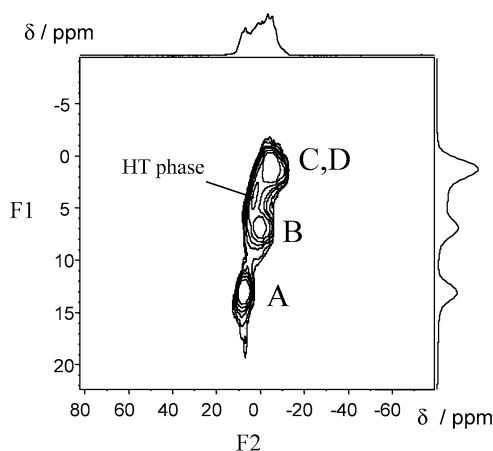


Figure 3. ^{23}Na MQMAS NMR spectrum of BOSO.

temperature (LT) phase (260 K) is characterized by an overlap of several components, producing a broad signal with some fine structure. Based on earlier ^{23}Na magic angle spinning (MAS) and double rotation (DOR) NMR work by Engelhardt and co-workers,¹² this spectrum of BOSO in the LT phase is expected to contain four lines, which are broadened by second-order quadrupolar interaction, which will be analyzed in more detail below. Gradual changes and narrowing of this spectrum occur upon increasing the temperature, and a narrow line results at 310 K. The different temperatures depicted in Figure 2 well document that the phase transition is not sharp; the observed changes rather occur over a temperature range of at least 50 K. As it seems at a first glance, the narrow ^{23}Na NMR line at 310 K could be an indication of high mobility. However, as will be shown below, this is not the case, and the sodium motion has to be analyzed in more detail with additional experiments.

The different components of the low-temperature sample at 260 K are better resolved in the ^{23}Na MQMAS NMR spectrum, which is plotted in Figure 3. The F1 dimension separates the different lines by their chemical shifts, which is composed of the isotropic and quadrupolar-induced shift contributions, but quadrupolar line broadening is eliminated. The F2 dimension

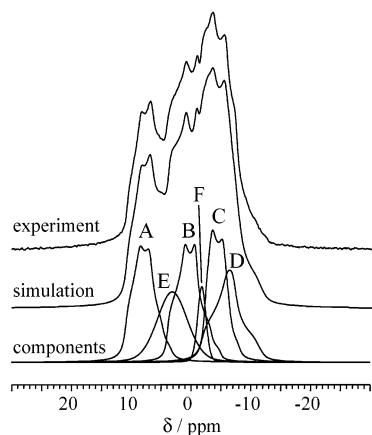


Figure 4. Simulation of the ^{23}Na MAS NMR spectra of BOSO at 260 K.

TABLE 1: Parameters Obtained by the Simulation of the ^{23}Na MAS NMR Spectrum of BOSO at 260 K

component	C_q (MHz)	η	δ_{iso} (ppm)	I (%)
A	1.45	0.55	11.1	20
B	1.55	0.60	4.1	21
C	1.30	0.35	-2.0	19
D	1.60	0.80	-1.8	19
E			3.1 ^a	16
F			-1.9 ^a	4

^a Apparent line positions not corrected for quadrupolar-induced shift.

includes the second-order quadrupolar line broadening under MAS conditions. From the comparison between our MQMAS NMR experiment (Figure 3) and DOR NMR results,¹² it must be concluded that the two components C and D (see Engelhardt et al.) are not resolved in Figure 3. A small impurity of the high-temperature (HT) phase can be observed, which is labeled in the figure. All of the information of the DOR and MQMAS experiments is compatible so that consistent starting values for a simulation of the MAS NMR experiment can be derived. A general guideline on how to combine the information from MAS, DOR, and MQMAS NMR experiments has been proposed by Engelhardt et al.¹³ The DOR (if carried out at different magnetic fields) and MQMAS experiments provide the isotropic chemical shift, δ_{cs} , and the second-order quadrupolar effect, $\text{SOQE} = C_q/(1 + \eta^2/3)^{1/2}$. Since they do not provide the asymmetry parameter of the electric field gradient, η , this parameter must be adjusted to fit the line shapes of the ^{23}Na MAS NMR spectrum. Figure 4 is the final result of the spectral decomposition, which describes the ^{23}Na MAS NMR spectrum of BOSO at 260 K by six components. These components can be rationalized as follows. Lines A, B, C, and D are the four components of BOSO in the LT phase. From this fit, it becomes clear that the two components, C and D, are difficult to resolve in the MQMAS NMR experiment at the magnetic field of 11.7 T. Line E is the impurity of the HT phase, which was also observed by Engelhardt et al.¹² at this temperature. Line F is consistent with a small impurity of the hydrosodalite $[\text{Na}_3(\text{H}_2\text{O})_4]_2[\text{Si}_6\text{Al}_6\text{O}_{24}]$.¹⁰ The parameters obtained by the spectral simulation of Figure 4 are collected in Table 1. The four components, A–D, of the LT phase of BOSO appear to have equal populations as expected from the crystal structure. It is very difficult to assign these components to the four sodium positions, because the quadrupole interaction parameters are very similar. Component A exhibits an isotropic chemical shift of 11.1 ppm, which is well separated from the other three components B–D (4.1, -2.0, and -1.8 ppm), which may

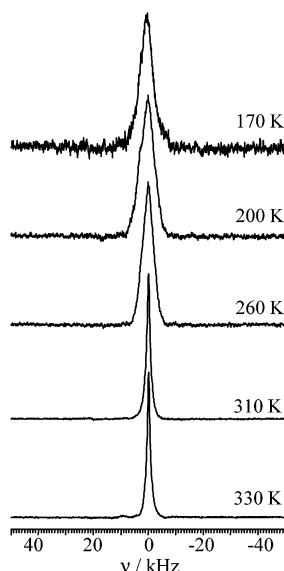


Figure 5. Stationary ^2H NMR spectra of BOSO at various temperatures.

indicate a special environment of the sodium cations that correspond to line A. A possible rationale for the component A being so special will be discussed below in context with motional models within the sodalite cage.

Next, the motion of the $\text{B}(\text{OH})_4^-$ anion above and below the phase transition is analyzed, using the well established ^2H NMR technique⁹ on stationary samples. To this end, BOSO has been prepared with fully deuterated tetrahydroxoborate anions. The ^2H quadrupole echo NMR spectra of this sample at temperatures ranging from 170 to 330 K are shown in Figure 5. The line observed at 170 K has a very unspecific shape, and the width of 62.2 kHz (full width at half-maximum) indicates that there must be already a considerable mobility at this low temperature.⁹ Upon increase of the temperature, the ^2H NMR line becomes even more narrow, especially around the phase transition at 303 K. Above the phase transition (310 K, 14.3 kHz), there is a virtually isotropic mobility of the tetrahydroxoborate ions. No further information on the motional mechanism can be gained from this ^2H NMR line shape analysis.

Another hint on a higher mobility of the $\text{B}(\text{OH})_4^-$ anions above the phase transition results from ^{11}B NMR spectra in Figure 6, which have been conducted so as to acquire the satellite transitions, $|\pm 3/2\rangle \leftrightarrow |\pm 1/2\rangle$ (SATRAS experiment). Figure 6a shows a spinning sideband pattern, covering a range consistent with a maximum quadrupole coupling constant, C_q , of 150–175 kHz for the LT phase. The high-temperature phase (Figure 6b) has a considerably narrower spinning sideband spectral distribution, indicating a maximum C_q value of 50 kHz. This reduced quadrupole coupling constant at the higher temperature is another indication for a higher motional degree of freedom of the $\text{B}(\text{OH})_4^-$ anion. Interestingly, a ^{23}Na NMR SATRAS experiment of the high-temperature phase (Figure 6c) shows spinning sidebands in a range that translates into a quadrupole coupling constant of 390 ± 15 kHz. An isotropic motion of the sodium ions would not be consistent with such a value. This observation is a first indication of a nonisotropic movement of the sodium ions.

The motion of the $\text{B}(\text{OH})_4^-$ anions is analyzed in more detail by the ^{11}B – ^1H REDOR technique, and the results are collected in Figure 7. The experimental ^{11}B – ^1H REDOR data of BOSO show a higher initial slope at 260 K compared to 320 K. This observation clearly shows that the additional motional degrees

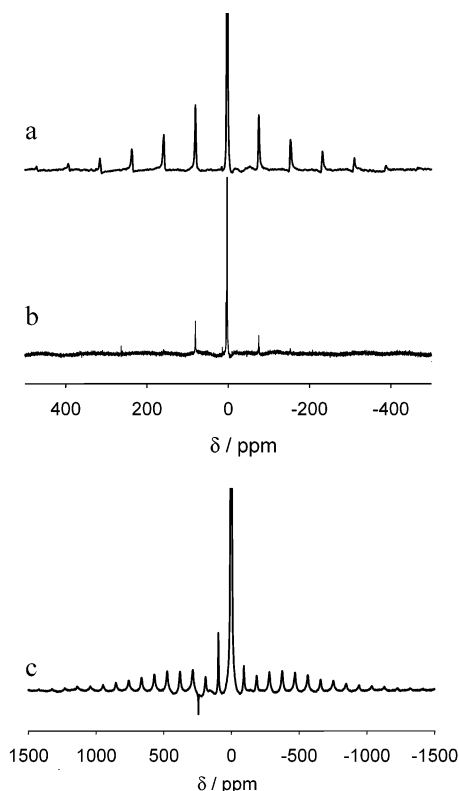


Figure 6. ^{11}B SATRAS NMR spectra of BOSO at (a) 260 and (b) 320 K and (c) ^{23}Na SATRAS NMR spectra of BOSO at 320 K. The central line has been cut after intensity magnification.

of freedom in the high-temperature phase, as observed by ^2H NMR, reduce the ^{11}B – ^1H dipolar interaction. Different motional scenarios were now considered, and the expected initial slopes of the REDOR curves (cf. Theoretical Section) have been predicted for them. An immobile system would produce a ^{11}B – ^1H second moment of $570.5 \times 10^6 \text{ rad}^2 \text{ s}^{-2}$, which is characterized by a rather steep slope of the REDOR curve, and the experimental data are clearly inconsistent with this model at both temperatures (static case in Figure 7). A rotation of the O–H bonds about the B–O axes (model I in Figure 7b) reduces the expected second moment to $324.5 \times 10^6 \text{ rad}^2 \text{ s}^{-2}$, which means that the REDOR curve labeled I in Figure 7 would be expected. This expected curve is still much steeper than the observed data. Now, in model II, the O–H rotation is combined with a two-site jump about the 2-fold axis of the tetrahydroxoborate anion, and an expected second moment of $83.7 \times 10^6 \text{ rad}^2 \text{ s}^{-2}$ results, but curve II is still too steep. A better agreement between the expected initial slope of the REDOR curve and the data collected at 260 K is achieved for model III (second moment of $34.6 \times 10^6 \text{ rad}^2 \text{ s}^{-2}$), which combines the O–H rotation with a rotation of the entire molecule about a 3-fold axis. The expected and observed initial slopes match reasonably well in the range $0 \leq \Delta S/S_0 \leq 0.2$. This rotation about a 3-fold axis means that one sodium ion is probably oriented close to the rotation axis of the tetrahedral anion, while the other three Na positions are close to the mobile part of $\text{B}(\text{OH})_4^-$. This model is supported by the fact that one ^{23}Na NMR chemical shift differs quite substantially from the other three (see above). The experimental data obtained in the high-temperature phase (320 K) match very well with a model where the $\text{B}(\text{OH})_4^-$ anion undergoes an isotropic local reorientation so that the intramolecular ^{11}B – ^1H dipolar interaction is completely averaged out and only weak intermolecular interactions between different

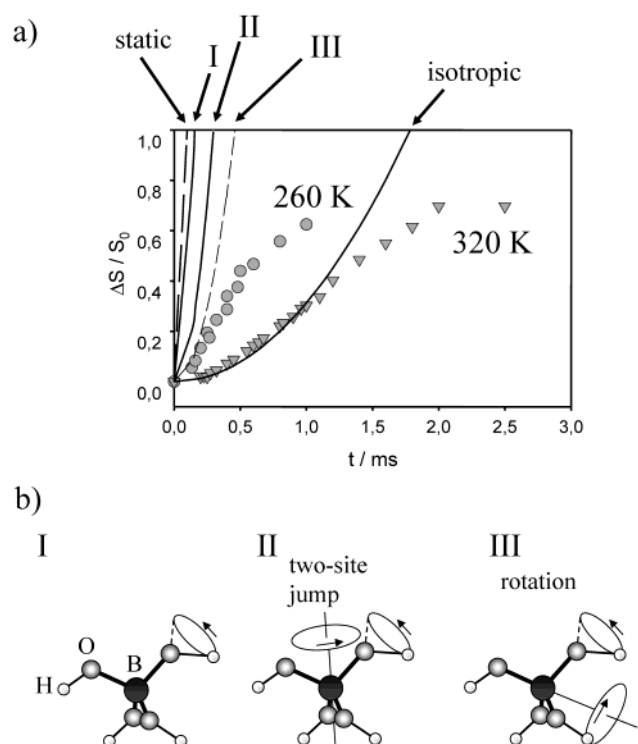


Figure 7. ^{11}B – ^1H REDOR data of BOSO and simulation with different motional models.

sodalite cages remain, yielding a second moment of $2.3 \times 10^6 \text{ rad}^2 \text{ s}^{-2}$. The dynamic reduction of the dipolar interactions can be restricted with a good approximation to intracage averaging because of the large distances between cage centers of ca. 7.8 Å from which small bite angles for relative motional effects result.

We now proceed to apply the REDOR technique to the motion of the sodium cations. However, since the ^{23}Na – ^{11}B dipolar system has two quadrupolar nuclei, the excitation behavior of the ^{11}B nuclei must be characterized first. It is not clear a priori which spin states ($|3/2\rangle$, $|1/2\rangle$, $|-1/2\rangle$, $|-3/2\rangle$) participate in the REDOR effect and to what extent. For the ^{11}B – ^1H experiment this was not a problem, because the ^1H nuclei have only one transition, that is, $|1/2\rangle \leftrightarrow |-1/2\rangle$. This problem has been addressed by a calibration of the ^{11}B excitation conditions with an experiment that uses the same ^{11}B pulse scheme as the ^{23}Na – ^{11}B REDOR experiment, namely, ^{27}Al – ^{11}B REDOR. The ^{27}Al and ^{11}B spins do not undergo a motion relative to each other because the aluminum is fixed in the sodalite framework and boron is captured at the center of the sodalite cage by steric effects. Since the ^{27}Al – ^{11}B second moment can be calculated from the crystal structure ($1.1 \times 10^6 \text{ rad}^2 \text{ s}^{-2}$), the expected slopes of the REDOR curves can be predicted for selective and nonselective ^{11}B excitation. Figure 8 shows the experimental and predicted REDOR data. The ^{27}Al – ^{11}B REDOR curve for the low-temperature phase at 260 K agrees very well with a predicted slope where only the ^{11}B central transition, $|1/2\rangle \leftrightarrow |-1/2\rangle$, is taken into account. On the other hand, all ^{11}B transitions, $|3/2\rangle \leftrightarrow |1/2\rangle$, $|1/2\rangle \leftrightarrow |-1/2\rangle$, $|-1/2\rangle \leftrightarrow |-3/2\rangle$, contribute to the REDOR effect at 320 K, since the corresponding predicted curve matches the experimental data very well. It is surprising that a relatively small difference in the ^{11}B quadrupole coupling constant (50 kHz at 320 K, 150–175 kHz at 260 K) can produce such a substantial difference in the ^{11}B excitation in the REDOR experiment. The ^{11}B nutation at 320 K is sinusoidal, and it confirms a liquidlike, nonselective

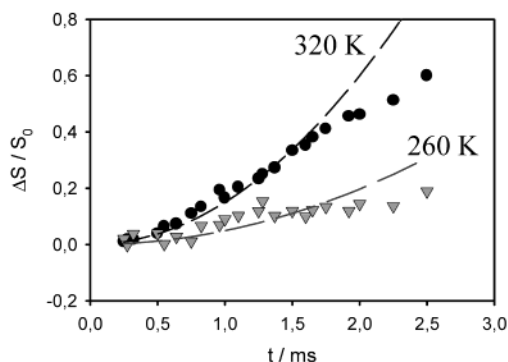


Figure 8. ^{27}Al – ^{11}B REDOR data of BOSO at 260 and 320 K and simulation with selective and nonselective ^{11}B excitation, respectively.

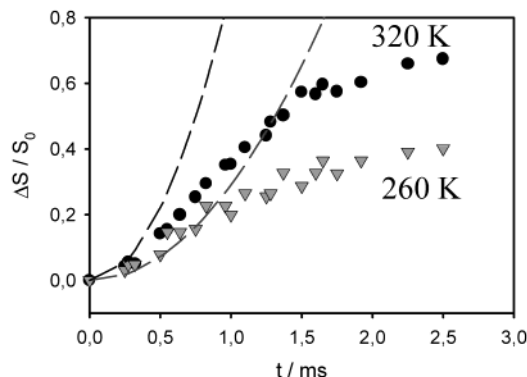


Figure 9. ^{23}Na – ^{11}B REDOR data of BOSO at 260 and 320 K and simulation with selective and nonselective ^{11}B excitation, respectively.

excitation. The ^{11}B nutation experiment at 260 K shows a shorter nutation period, which is more solidlike, but it does not correspond to fully selective excitation. However, it must be considered that the REDOR experiment applies a train of 180° pulses, while the nutation experiment only uses one pulse with varying length. It has not been investigated how the application of many 180° pulses have an accumulating effect on the excitation selectivity of quadrupolar nuclei in a REDOR experiment. Here, we have simply circumvented this problem by calibrating the excitation experimentally by performing the REDOR experiment on the ^{27}Al – ^{11}B spin system. With this information, the ^{23}Na – ^{11}B REDOR data can now be analyzed in terms of motional effects.

The ^{23}Na – ^{11}B REDOR data are shown in Figure 9. The ^{11}B pulses in these experiments have been calibrated exactly under the same power conditions as in the subsequent ^{27}Al – ^{11}B experiment. Therefore, the ^{11}B excitation conditions are identical in both. It is striking that the data obtained at 320 K reveal a higher slope, implying a stronger dipolar interaction. This is of course, at a first glance, unexpected, if additional motion of whatever type sets in at the higher temperature. However, as has been explained above, the contribution of the different ^{11}B transitions to the REDOR effect change at the phase transition, and at the higher temperature, the additional contribution of the $|\pm 3/2\rangle$ spin states increases the sensitivity of the experiment (see Theoretical Section), which produces the increased slope of the REDOR curve.

The broken lines in Figure 9 show the expected initial slopes of the ^{23}Na – ^{11}B REDOR curves for the low-temperature (260 K) and high-temperature (320 K) ^{11}B excitation, which is selective and nonselective, respectively, according to the above analysis using ^{27}Al – ^{11}B REDOR. These expected curves have both been calculated with a ^{23}Na – ^{11}B second moment of 6.56

$\times 10^6 \text{ rad}^2 \text{ s}^{-2}$, which was calculated from the (rigid) crystal structure. A closer inspection of the observed and expected initial slopes shows that the agreement is excellent for the low-temperature phase at 260 K (for $0 \leq \Delta S/S_0 \leq 0.2$). In contrast, the expected slope for rigid sodium cations is much steeper for the HT phase (320 K) than actually observed in the experiment. This observation is a clear indication of motional averaging of the heteronuclear ^{23}Na – ^{11}B dipolar interaction in the HT phase but not in the LT phase. However, the reduction factor in the HT phase is not large. A reduced second moment of $4.0 \times 10^6 \text{ rad}^2 \text{ s}^{-2}$ would fit with the experimental data of the HT phase. Thus, either the motion must have a rather small amplitude or only a few spin pairs are in a dynamic situation while others are rigid (dynamic heterogeneity). Finally, the ^{23}Na – ^{11}B REDOR data in the HT phase clearly do not confirm a nearly isotropic motion, which one might have concluded from the narrow ^{23}Na NMR line width at 310 K (Figure 2).

Conclusions

It was shown that the REDOR technique can be applied to multispin systems, even when quadrupolar nuclei are involved, and it is suitable to provide information on ionic mobility. These REDOR data clearly show that the additional degree of freedom in the motion of the $\text{B}(\text{OH})_4^-$ anion in tetrahydroxoborate sodalite is accompanied by an onset of cation motion (motional coupling). However, the sodium motion is far from being isotropic, and it is rather better characterized by local, anisotropic jump processes. The combination of NMR techniques presented here is proposed as a tool to investigate the details of ionic motion in rotor phases. The described NMR methods provide a great deal of structural details for which traditional X-ray diffraction methods are largely insensitive. Diffraction methods cannot distinguish between the type of disorder (static or dynamic), and space group symmetries are higher than the local, disordered structure.

Acknowledgment. This work was supported by the Deutsche Forschungsgemeinschaft (Grant SFB 458). The authors thank Professor Hellmut Eckert at Westfälische Wilhelms-Universität Münster for access to the NMR facilities and for valuable discussions.

References and Notes

- (1) Holm Kristensen, J.; Farnan, I. *J. Magn. Reson.* **2002**, *158*, 99.
- (2) Witschas, M.; Eckert, H.; Wilmer, D.; Banhatti, R. D.; Funke, K.; Fitter, J.; Lechner, R. E.; Korus, G.; Jansen, M. *Z. Phys. Chem.* **2000**, *214*, 643.
- (3) Buhl, J. C.; Mundus, C.; Löns, J.; Hoffmann, W. *Z. Naturforsch.* **1994**, *49a*, 1171.
- (4) Gullion, T.; Schaefer, J. *J. Magn. Reson.* **1989**, *81*, 196.
- (5) Bertmer, M.; Eckert, H. *Solid State Nucl. Magn. Reson.* **1999**, *15*, 139.
- (6) Mueller, K. T. *J. Magn. Reson. A* **1995**, *113*, 81.
- (7) Schmidt, A.; McKay, R. A.; Schaefer, J. *J. Magn. Reson.* **1992**, *96*, 644.
- (8) Hudalla, C.; Eckert, H.; Dupree, R. *J. Phys. Chem.* **1996**, *100*, 15986.
- (9) Schmidt-Rohr, K.; Spiess, H. W. *Multidimensional Solid-State NMR and Polymers*; Academic Press: London, 1994.
- (10) Sieger, P. Doctoral Dissertation, Universität Konstanz, Germany, 1994.
- (11) (a) Medek, A.; Harwood, J. S.; Frydman, L. *J. Am. Chem. Soc.* **1995**, *117*, 12779. (b) Fernandez, C.; Amoureux, J. P. *Chem. Phys. Lett.* **1995**, *242*, 449.
- (12) Engelhardt, G.; Sieger, P.; Felsche, J. *Anal. Chim. Acta* **1993**, *283*, 967.
- (13) Engelhardt, G.; Kentgens, A. P. M.; Koller, H.; Samoson, A. *Solid State Nucl. Magn. Reson.* **1999**, *15*, 171.